AD-A073 456 ARMY MISSILE RESEARCH AND DEVELOPMENT COMMAND REDSTO--ETC F/G 20/4
REAL TIME DIGITAL MODEL OF A ROLLING AIRFRAME.(U)
JUL 78 V S GRIMES

UNCLASSIFIED DRDMI-T-78-75 NL

1 OF 1

AD
A073456

END
DATE
FILMED
10-79
DDC

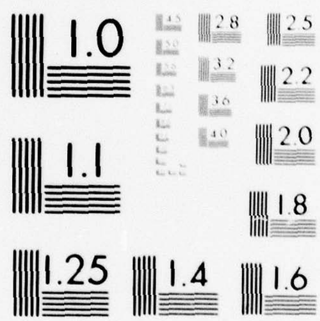

MICROCOPY RESOLUTION TEST CHART
NATIONAL BUREAU OF STANDARDS-1963-A

TECHNICAL REPORT T-78-75

REAL TIME DIGITAL MODEL OF A ROLLING AIRFRAME

Victor S. Grimes, Jr.
Systems Simulation Directorate
Technology Laboratory

31 July 1978

Approved for Public Release; Distribution Unlimited.

U.S. ARMY MISSILE RESEARCH AND DEVELOPMENT COMMAND

Redstone Arsenal, Alabama 35809

DMI FORM 1000, 1 APR 77

DISPOSITION INSTRUCTIONS

DESTROY THIS REPORT WHEN IT IS NO LONGER NEEDED. DO NOT RETURN IT TO THE ORIGINATOR.

DISCLAIMER

THE FINDINGS IN THIS REPORT ARE NOT TO BE CONSTRUED AS AN OFFICIAL DEPARTMENT OF THE ARMY POSITION UNLESS SO DESIGNATED BY OTHER AUTHORIZED DOCUMENTS.

TRADE NAMES

USE OF TRADE NAMES OR MANUFACTURERS IN THIS REPORT DOES NOT CONSTITUTE AN OFFICIAL ENDORSEMENT OR APPROVAL OF THE USE OF SUCH COMMERCIAL HARDWARE OR SOFTWARE.

UNCLASSIFIED

SECURITY CLASSIFICATION OF THIS PAGE (When Data Entered)

(14)

REPORT DOCUMENTATION PAGE		READ INSTRUCTIONS BEFORE COMPLETING FORM
1. REPORT NUMBER: DRDMI- T-78-75	2. GOVT ACCESSION NO.	3. RECIPIENT'S CATALOG NUMBER (9)
4. TITLE (and Subtitle): (6) Real Time Digital Model of a Rolling Airframe.		5. TYPE OF REPORT & PERIOD COVERED: Technical Report.
		6. PERFORMING ORG. REPORT NUMBER
7. AUTHOR(s): (10) Victor S. Grimes, Jr.		8. CONTRACT OR GRANT NUMBER(s): (16) 1X464306D646 644306.6460012
9. PERFORMING ORGANIZATION NAME AND ADDRESS: Commander, US Army Missile Research and Development Command, ATTN: DRDMI-TD, Redstone Arsenal, Alabama 35809		10. PROGRAM ELEMENT, PROJECT, TASK AREA & WORK UNIT NUMBERS
11. CONTROLLING OFFICE NAME AND ADDRESS: Commander, US Army Missile Research and Development Command, ATTN: DRDMI-TI, Redstone Arsenal, Alabama 35809		12. REPORT DATE: (11) 31 July 1978
		13. NUMBER OF PAGES: 49 (12) 53p.
14. MONITORING AGENCY NAME & ADDRESS (if different from Controlling Office)		15. SECURITY CLASS. (of this report): UNCLASSIFIED
		15a. DECLASSIFICATION/DOWNGRADING SCHEDULE

16. DISTRIBUTION STATEMENT (of this Report)

Approved for public release, distribution unlimited.

17. DISTRIBUTION STATEMENT (of the abstract entered in Block 20, if different from Report)

18. SUPPLEMENTARY NOTES

19. KEY WORDS (Continue on reverse side if necessary and identify by block number)

real time simulation	convolution	Euler Tunable Convolution (ETC)
IRSS	numerical convolution	
digital model	tunable integration	Laplace transforms
digital simulation	airframe equations	HWIL
Z transforms	coupled differential equations	closed loop

20. ABSTRACT (Continue on reverse side if necessary and identify by block number)

An all-digital airframe model of a rolling missile is developed by using tunable convolution and integration techniques. The model is capable of handling high frequency airframe dynamics in real time with large time steps and hardware in the loop (HWIL). This model is currently in use in three applications at the MIRADCOM Advanced Simulation Center in Aeroballistics Directorate, Technology Laboratory.

(Continued)

DD FORM 1473, 1 JAN 73 EDITION OF 1 NOV 65 IS OBSOLETE

UNCLASSIFIED

SECURITY CLASSIFICATION OF THIS PAGE (When Data Entered)

79 08 31 022

393 427

19. KEY WORDS (Continued)

nonlinear differential equations
open loop
recurrence equations

TABLE OF CONTENTS

LIST OF ILLUSTRATIONS

1. INTRODUCTION

The initial simulation research work done in the MIRADCOM Infrared Simulation System (IRSS) was heavily partitioned between analog and digtial computers that were driving real time hardware [1]. Several disadvantages to this method of driving the IRSS hardware were noted. These disadvantages centered primarily on the complexity and maintenance of such a distributed system and on the resulting control difficulties. It also became apparent that complexity, maintenance, and these control difficulties could be significantly reduced by placing all computer functions external to the IRSS in one existing high speed digital computer that communicated with the IRSS facility.

Only one problem remained before this idea could be implemented. **The airframe solution frequencies were too high for conventional** real-time digital simulation methods. This report documents the modeling method that was discovered to be suitable for solving this problem.

2. AIRFRAME EQUATIONS

The airframe equations originally developed for analog and hybrid simulation are suitable for digital simulation with minor modification. These equations can be reduced to

$$\dot{u}' = \xi_{14} + v'r' - w'q' - \xi_{18} \sin (\theta_L + \theta_P) \tag{1}$$

$$\dot{v}' = \xi_5 v' - \xi_6 r' + \xi_{21} \delta_{wi} \sin\phi \tag{2}$$

$$\dot{w}' = \xi_5 w' + \xi_6 q' + \xi_{18} \cos (\theta_L + \theta_P) - \xi_{21} \delta_{wi} \cos\phi \tag{3}$$

$$\dot{q}' = \xi_1 w' + \xi_2 q' + \xi_{20} \delta_{wi} \cos\phi \tag{4}$$

$$\dot{r}' = - \xi_1 v' + \xi_2 r' + \xi_{20} \delta_{wi} \sin\phi \tag{5}$$

in the non-rolling missile coordinate system shown in Figure 1. Utility definitions used in Equations (1) through (5) are

$$\xi_1 = \frac{\rho S u'}{2I_y} \left[dCm^*_{total} + (X_{CG} - X_R)\, Cn^*_{total} \right] \tag{6}$$

$$\xi_2 = \frac{\rho S u' d^2}{2I_y} Cm_q \tag{7}$$

$$\xi_5 = - \frac{\rho S u'}{2m} Cn^*_{total} \tag{8}$$

$$\xi_6 = u' \tag{9}$$

$$\xi_{18} = g = 32.174 \text{ ft/sec}^2 \tag{10}$$

$$\xi_{20} = 3.81972 \left[\beta_{10}(G_1 + G_2\alpha) + \beta_{11}(g_1 + g_2\alpha) \right] \tau_m \tag{11}$$

$$\xi_{21} = - 3.81972\, \beta_5(g_1 + g_2\alpha)\, \tau_m \tag{12}$$

$$\beta_1 = \frac{\rho S u'}{2} \tag{13}$$

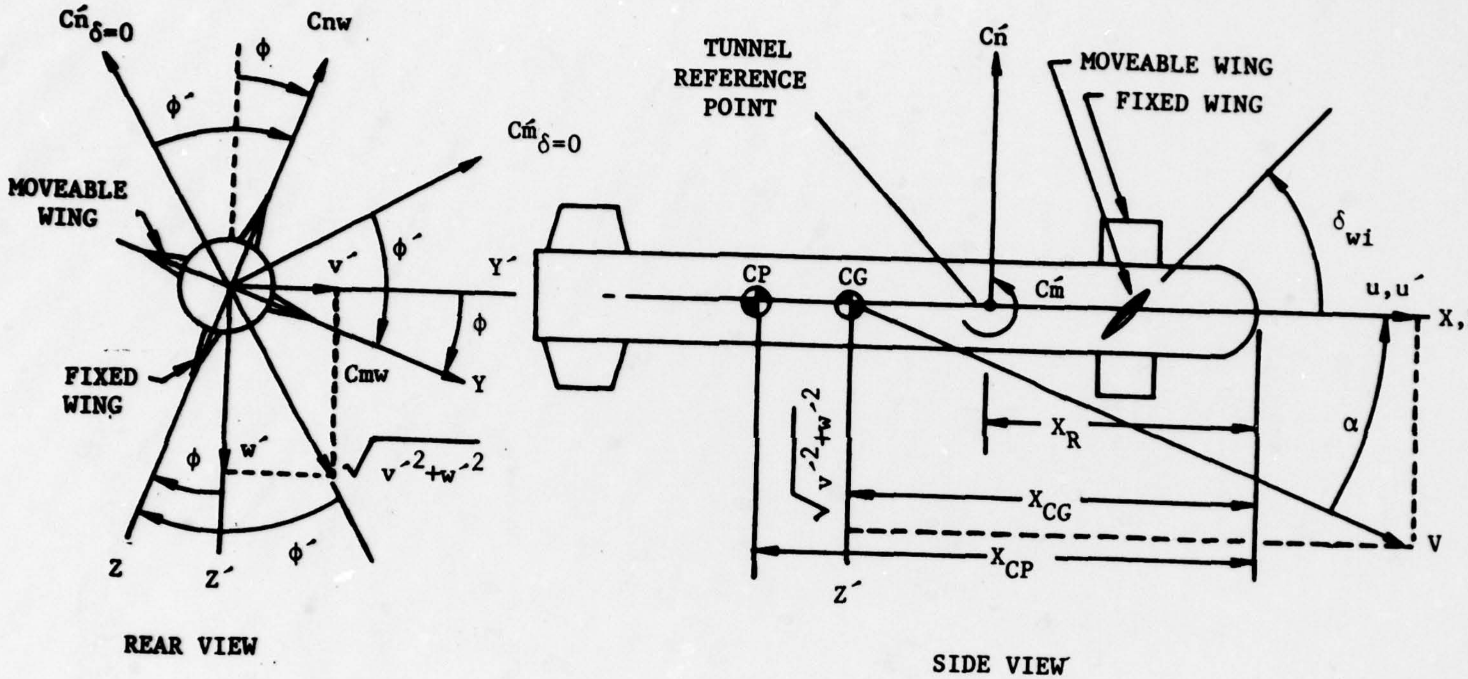

(X,Y,Z) axes are missile fixed with origin at GC.
(X´,Y´,Z´) axes are nonrolling but do pitch and yaw with the missile. The Y´ axis is always in a moving plane horizontal with respect to earth.

Figure 1. Missile coordinate systems and aerodynamic moments and normal forces.

$$\beta_2 = \beta_1 \, (1/I_y) \tag{14}$$

$$\beta_4 = - \beta_1 \, (1/m) \tag{15}$$

$$\beta_5 = \beta_4 \, u' \tag{16}$$

$$\beta_6 = \beta_2 \, u' \tag{17}$$

$$\beta_8 = \beta_2 \, (X_{CG} - X_R) \tag{18}$$

$$\beta_{10} = \beta_6 \, d \tag{19}$$

$$\beta_{11} = \beta_8 \, u' \tag{20}$$

$$\xi_{14} = T_h \, (1/m) + \beta_5 \, C_A \tag{21}$$

$$Cm^*_{total} = Cm^* + Cm_{pe} \tag{22}$$

$$Cn^*_{total} = Cn^* + Cn_{pe} \tag{23}$$

$$Cm^* = F_1 + F_2\alpha + (F_3 + F_4\alpha) \, |\delta_{wi}| \, \tau_m \tag{24}$$

$$Cn^{*} = f_1 + f_2\alpha + (f_3 + f_4\alpha)|\delta_{wi}|\tau_m \tag{25}$$

$$C_A = C_{D_o} + \Delta C_A \tag{26}$$

$$\Delta C_A = (A_1 + A_2\alpha)|\delta_{wi}| \tag{27}$$

where τ_m is a wing incidence control tuning factor that must be determined by tuning to match test flight maneuverability in conjunction with τ_{CP} which is an indirect measure of CP location that must also be tuned for matching test flight trim conditions.

τ_{CP} is implemented in

$$(X_{CG} - X_R) = (X_{CG} - X_R)_{TABLE} + \tau_{CP} \quad . \tag{28}$$

Note that Equations (1) through (5) are coupled, nonlinear, and time-varying. Additional equations for use in the airframe model are

$$\phi = \int p' dt \tag{29}$$

$$\theta_P \simeq \int q' dt \tag{30}$$

$$\psi_P \simeq \int \frac{r'}{\cos\theta_P} dt \tag{31}$$

where p' is a roll-rate time history from a nominal test flight.

3. MODEL DEVELOPMENT

Consider coupled Equations (3) and (4) together.

$$\dot{q}' = \xi_1 w' + \xi_2 q' + \xi_{20} \delta_{wi} \cos\phi \quad (32)$$

$$\dot{w}' = \xi_5 w' + \xi_6 q' + \xi_{18} \cos(\theta_L + \theta_P) - \xi_{21} \delta_{wi} \cos\phi \quad (33)$$

Take the Laplace transforms of Equations (32) and (33), and assume constant coefficients to obtain,

$$q'(s) = [q'(o) + \xi_1 w'(s) + \xi_{20} L(\delta_{wi} \cos\phi)]/(s - \xi_2) \quad (34)$$

and

$$w'(s) = \{w'(o) + \xi_6 q'(s) + L[\xi_{18} \cos(\theta_L + \theta_P)$$

$$- \xi_{21} \delta_{wi} \cos\phi]\}/(s - \xi_5) \quad (35)$$

after rearrangement. The coupling is shown in Figure 2. Take the Z-transform of Equation (34) as

$$q'(z) = q'(o) \mathbf{Z}\left(\frac{1}{s - \xi_2}\right) + \xi_1 \mathbf{Z}\left[w'(s) \left(\frac{1}{s - \xi_2}\right)\right]$$

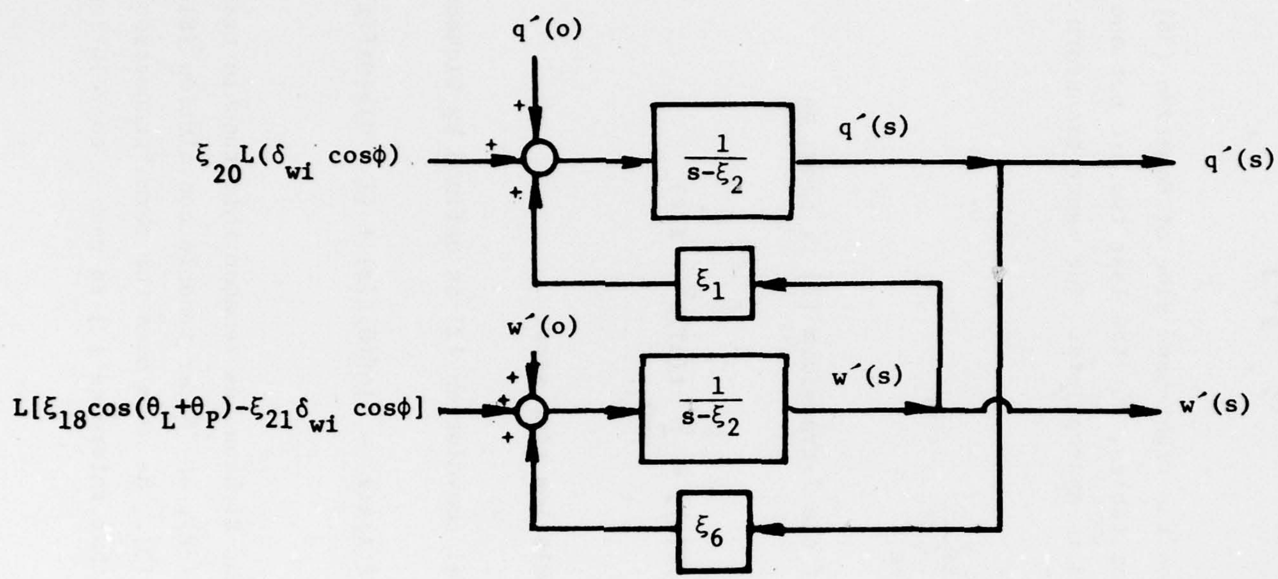

Figure 2. q´ and w´ coupling diagram.

$$+ \xi_{20} \mathcal{Z}\left[L\,(\delta_{wi}\cos\phi)\left(\frac{1}{s - \xi_2}\right)\right] \tag{36}$$

The first Z-transform on the right-hand side of Equation (36) is exact and can be obtained from tables, but the last two are not and an approximate convolution method is appropriate. The exact transform is

$$\mathcal{Z}\left(\frac{1}{s - \xi_2}\right) = \frac{1}{1 - ze^{\xi_2 T}} \tag{37}$$

where the definition of the Z-transform [2] is taken as

$$\mathcal{Z}\{L[f(t)]\} = \mathcal{Z}[f(s)] = \sum_{n=0}^{\infty} f(nT)z^n = f(z) \tag{38}$$

Note that T is the simulation time step.

Tunable trapezoidal convolution [2] is defined by Dickson as

$$\mathcal{Z}[f(s)g(s)] \simeq Tf(z)g(z) - T[\eta f(0)g(z) + (1 - \eta)g(0)f(z)] \tag{39}$$

One should be aware that Dickson has renamed this tunable trapezoidal convolution, Equation (39), as "Euler tunable convolution (ETC)" in a more recent reference [3]. He also uses the term "trapezoidal tunable convolution (TTC)" in that reference [3] to name a convolution method not used in this work.

If Equation (39) is applied to the middle RHS term of Equation (36),

$$\mathcal{Z}\left[w'(s)\left(\frac{1}{s-\xi_2}\right)\right] \simeq Tw'(z)\left(\frac{1}{1-ze^{\xi_2 T}}\right) - T\eta w'(0)\left(\frac{1}{1-ze^{\xi_2 T}}\right)$$

$$- T(1-\eta)L^{-1}\left(\frac{1}{s-\xi_2}\right)_{t=0} w'(z) \tag{40}$$

Note that

$$L^{-1}\left(\frac{1}{s-\xi_2}\right)_{t=0} = 1 \tag{41}$$

from the transform table in the Appendix. Equation (40) becomes

$$\mathcal{Z}\left[w'(s)\left(\frac{1}{s-\xi_2}\right)\right] \simeq \frac{Tw'(z)}{1-ze^{\xi_2 T}} - \frac{T\eta w'(0)}{1-ze^{\xi_2 T}} - T(1-\eta)w'(z)\ . \tag{42}$$

If Equation (39) is applied to the last RHS term of Equation (36),

$$\mathcal{Z}\left[L(\delta_{wi}\cos\phi)\left(\frac{1}{s-\xi_2}\right)\right] \simeq T\left[\mathcal{Z}(\delta_{wi}\cos\phi)\right]\left(\frac{1}{1-ze^{\xi_2 T}}\right)$$

$$- T\eta(\delta_{wi}\cos\phi)_{t=0}\left(\frac{1}{1-ze^{\xi_2 T}}\right)$$

$$- T(1-\eta)\, L^{-1}\left(\frac{1}{s-\xi_2}\right)_{t=0} \mathcal{Z}(\delta_{wi}\cos\phi)$$

(43)

$$\mathcal{Z}\left[L(\delta_{wi}\cos\phi)\left(\frac{1}{s-\xi_2}\right)\right] \simeq \frac{T\,\mathcal{Z}(\delta_{wi}\cos\phi)}{1-ze^{\xi_2 T}} - \frac{T\eta(\delta_{wi}\cos\phi)_{t=0}}{1-ze^{\xi_2 T}}$$

$$- T(1-\eta)\,\mathcal{Z}(\delta_{wi}\cos\phi) \quad . \qquad (44)$$

Substitute Equations (37), (42), and (44) into Equation (36).

$$q'(z) \simeq \frac{q'(o)}{1-ze^{\xi_2 T}} + \xi_1\left[\frac{Tw'(z)}{1-ze^{\xi_2 T}} - \frac{T\eta w'(o)}{1-ze^{\xi_2 T}} - T(1-\eta)w'(z)\right]$$

$$+ \xi_{20}\left[\frac{T\,\mathcal{Z}(\delta_{wi}\cos\phi)}{1-ze^{\xi_2 T}} - \frac{T\eta(\delta_{wi}\cos\phi)_{t=0}}{1-ze^{\xi_2 T}} - T(1-\eta)\mathcal{Z}(\delta_{wi}\cos\phi)\right]$$

(45)

$$q'(z) \simeq \frac{q'(o) + \xi_1 T[w'(z) - \eta w'(o) - (1-\eta)(1-ze^{\xi_2 T})\, w'(z)]}{1-ze^{\xi_2 T}}$$

$$+ \frac{\xi_{20}T\left[\mathcal{Z}(\delta_{wi}\cos\phi) - \eta(\delta_{wi}\cos\phi)_{t=0} - (1-\eta)(1-ze^{\xi_2 T})\,\mathcal{Z}(\delta_{wi}\cos\phi)\right]}{1-ze^{\xi_2 T}}$$

(46)

From Equation (38), it is seen that

$$w'(z) = \sum_{n=0}^{\infty} w'(nT)\,z^n \tag{47}$$

and

$$\mathbf{Z}(\delta_{wi}\ \cos\phi) = \sum_{n=0}^{\infty} [\delta_{wi}\ (nT)\ \cos(\omega nT)]\,z^n \tag{48}$$

and

$$q'(z) = \sum_{n=0}^{\infty} q'(nT)\,z^n \quad . \tag{49}$$

Substitute Equations (47), (48), and (49) into Equation (46);

$$\begin{aligned}\left(1 - ze^{\xi_2 T}\right)\sum_{n=0}^{\infty} q'(nT)\ z^n \simeq q'(o) + \xi T\ &\Bigg[\sum_{n=0}^{\infty} w'(nT)z^n - \eta w'(o) \\ &- (1-\eta)\left(1 - ze^{\xi_2 T}\right)\sum_{n=0}^{\infty} w'(nT)z^n\Bigg] \\ &+ \xi_{20}T\Bigg\{\sum_{n=0}^{\infty} [\delta_{wi}\ (nT)\ \cos(\omega nT)]\,z^n \\ &- \eta(\delta_{wi}\ \cos\phi)_{t=0}\end{aligned}$$

$$- (1 - \eta)\left(1 - ze^{\xi_2 T}\right) \sum_{n=0}^{\infty} [\delta_{wi}(nT) \cos(\omega nT)] z^n \Bigg\}$$

(50)

$$\sum_{n=0}^{\infty} q'(nT)z^n - e^{\xi_2 T} \sum_{n=0}^{\infty} q'(nT)z^{n+1}$$

$$\simeq q'(o) + \xi_1 T[1 - (1 - \eta)] \sum_{n=0}^{\infty} w'(nT)z^n - \xi_1 T\eta w'(o)$$

$$+ \xi_1 T(1 - \eta)\, e^{\xi_2 T} \sum_{n=0}^{\infty} w'(nT)z^{n+1}$$

$$+ \xi_{20} T[1 - (1 - \eta)] \sum_{n=0}^{\infty} [\delta_{wi}(nT) \cos(\omega nT)]z^n$$

$$- \xi_{20} T\eta(\delta_{wi} \cos\phi)_{t=0}$$

$$+ \xi_{20} T(1 - \eta)e^{\xi_2 T} \sum_{n=0}^{\infty} [\delta_{wi}(nT) \cos(\omega nT)]z^{n+1} \quad (51)$$

Now the Z-transform shifting theorem consistent with the definition of Equation (38) is

$$z^{m}f(z) = \sum_{n=0}^{\infty} f(nT - mT) z^{n} - \sum_{n=0}^{m-1} f(nT - mT)\, z^{n} \tag{52}$$

where

$$m > 0 \tag{53}$$

and m is an integer. The shifting theorem, Equation (52), can also be written as

$$\sum_{n=0}^{\infty} f(nT)\, z^{n+m} = \sum_{n=m}^{\infty} f(nT - mT)\, z^{n} \tag{54}$$

which is directly useful in many cases. Use the shifting theorem, Equation (54), in Equation (51).

$$\sum_{n=0}^{\infty} q'(nT)\, z^{n} - e^{\xi_2 T} \sum_{n=1}^{\infty} q'(nT - T)\, z^{n}$$

$$\simeq q'(o) - \xi_1 T\eta w'(o) - \xi_{20} T\eta(\delta_{wi} \cos\phi)_{t=0}$$

$$+ \xi_1 T\eta \sum_{n=0}^{\infty} w'(nT)\, z^{n} + \xi_1 T(1-\eta)\, e^{\xi_2 T} \sum_{n-1}^{\infty} w'(nT - T)\, z^{n}$$

$$+ \xi_{20} T\eta \sum_{n=0}^{\infty} [\delta_{wi}\, (nT) \cos (\omega nT)]\, z^{n}$$

$$+ \xi_{20}T(1 - \eta)\, e^{\xi_2 T} \sum_{n=1}^{\infty} \{\delta_{wi}(nT - T) \cos [\omega(nT - T)]\}z^n \tag{55}$$

Complete all Z-transforms in Equation (55).

$$\left[\sum_{n=0}^{\infty} q'(nT)\, z^n - e^{\xi_2 T} \sum_{n=0}^{\infty} q'(nT - T)\, z^n + e^{\xi_2 T} q'(-T)\right]$$

$$\approx \Bigg\{ q'(o) - T\eta \left[\xi_1 w'(o) + \xi_{20}\, (\delta_{wi} \cos\phi)_{t=0}\right]$$

$$+ \xi_1 T\eta \sum_{n=0}^{\infty} w'(nT)\, z^n + \xi_1 T(1 - \eta)\, e^{\xi_2 T} \sum_{n=0}^{\infty} w'(nT - T)\, z^n$$

$$- \xi_1 T(1 - \eta)\, e^{\xi_2 T} w'(-T) + \xi_{20} T\eta \sum_{n=0}^{\infty} [\delta_{wi}(nT) \cos (\omega nT)]\, z^n$$

$$+ \xi_{20}T(1 - \eta)\, e^{\xi_2 T} \sum_{n=0}^{\infty} \{\delta_{wi}(nT - T) \cos [\omega(nT - T)\}z^n$$

$$- \xi_{20}T(1 - \eta)\, e^{\xi_2 T} [\delta_{wi}(-T) \cos(-\omega T)] \Bigg\} \tag{56}$$

The ability of Equation (56) to handle a nonzero initial condition can be shown by letting

$$n = 0 \tag{57}$$

and noting that

$$q'(o) = q'(o) \tag{58}$$

results when coefficients of z^n are equated.

Now let

$$n = 1 \tag{59}$$

and equate coefficients of z^n in Equation (56) to obtain

$$q'(T) \simeq e^{\xi_2 T} q'(o) + \xi_1 T(1-\eta) e^{\xi_2 T} w'(o)$$

$$+ \xi_{20} T(1-\eta) e^{\xi_2 T} [\delta_{wi}(o) \cos(o)]$$

$$+ \xi_1 T\eta w'(T) + \xi_{20} T\eta [\delta_{wi}(T) \cos(\omega T)] \quad . \tag{60}$$

If one lets

$$n = 2 \tag{61}$$

and equates coefficients of z^n in Equation (56), then

$$q'(2T) \simeq e^{\xi_2 T} q'(T) + \xi_1 T(1-\eta) e^{\xi_2 T} w'(T)$$

$$+ \xi_{20} T(1-\eta) e^{\xi_2 T} [\delta_{wi}(T) \cos(\omega T)] + \xi_1 T\eta w'(2T)$$

$$+ \xi_{20} T\eta [\delta_{wi}(2T) \cos(2\omega T)] \quad . \tag{62}$$

Comparison of Equations (60) and (62) shows that for

$$n \geq 1 \tag{63}$$

the coupled general recurrence equation is

$$q'_n \simeq e^{\xi_2 T} q'_{n-1} + \xi_1 T\eta w'_n + \xi_1 T(1 - \eta)e^{\xi_2 T} w'_{n-1}$$

$$+ \xi_{20} T\eta(\delta_{wi} \cos\phi)_n + \xi_{20} T(1 - \eta)e^{\xi_2 T} (\delta_{wi} \cos\phi)_{n-1} \quad . \tag{64}$$

If an identical procedure is used on Equation (35), one obtains the other coupled general recurrence equation,

$$w'_n \simeq e^{\xi_5 T} w'_{n-1} + \xi_6 T\eta q'_n + \xi_6 T(1 - \eta)e^{\xi_5 T} q'_{n-1} .$$

$$+ T\eta[\xi_{18} \cos(\theta_L + \theta_p) - \xi_{21}\delta_{wi} \cos\phi]_n$$

$$+ T(1 - \eta)e^{\xi_5 T} [\xi_{18} \cos(\theta_L + \theta_p) - \xi_{21}\delta_{wi} \cos\phi]_{n-1} \tag{65}$$

for

$$n \geq 1 \tag{66}$$

Also, if

$$n = 0 \tag{67}$$

the result is

$$w'(o) = w'(o) \tag{68}$$

for handling nonzero initial conditions.

Equations (64) and (65) are algebraic equations that can be solved simultaneously for q_n' and w_n'. The results are

$$q_n' \simeq \left[\frac{e^{\xi_2 T} + \xi_1\xi_6 T^2(1-\eta)\eta e^{\xi_5 T}}{1 - \xi_1\xi_6 T^2\eta^2}\right] q_{n-1}'$$

$$+ \frac{\xi_1 T\left[\eta e^{\xi_5 T} + (1-\eta)e^{\xi_2 T}\right]}{1 - \xi_1\xi_6 T^2\eta^2} w_{n-1}' + \left(\frac{\xi_1\xi_{18} T^2\eta^2}{1 - \xi_1\xi_6 T^2\eta^2}\right)\cos(\theta_L + \theta_P)_n$$

$$+ \left[\frac{\xi_1\xi_{18} T^2 (1-\eta)\eta e^{\xi_5 T}}{1 - \xi_1\xi_6 T^2\eta^2}\right]\cos(\theta_L + \theta_P)_{n-1}$$

$$+ \left[\frac{T_\eta(\xi_{20} - \xi_1\xi_{21} T\eta)}{1 - \xi_1\xi_6 T^2\eta^2}\right](\delta_{wi}\cos\phi)_n$$

$$+ \left[\frac{T(1-\eta)\left(\xi_{20} e^{\xi_2 T} - \xi_1\xi_{21} T\eta e^{\xi_5 T}\right)}{1 - \xi_1\xi_6 T^2\eta^2}\right](\delta_{wi}\cos\phi)_{n-1} \tag{69}$$

and

$$w'_n \simeq \left[\frac{e^{\xi_5 T} + \xi_1\xi_6 T^2(1-\eta)\eta e^{\xi_2 T}}{1 - \xi_1\xi_6 T^2\eta^2}\right] w'_{n-1} + \frac{\xi_6 T\left[\eta e^{\xi_2 T} + (1-\eta)e^{\xi_5 T}\right]}{1 - \xi_1\xi_6 T^2\eta^2}\, q'_{n-1}$$

$$+ \left(\frac{\xi_{18} T\eta}{1-\xi_1\xi_6 T^2\eta^2}\right)\cos\,(\theta_L + \theta_P)_n + \left[\frac{\xi_{18} T(1-\eta)e^{\xi_5 T}}{1 - \xi_1\xi_6 T^2\eta^2}\right]\cos\,(\theta_L + \theta_P)_{n-1}$$

$$+ \left[\frac{T\eta(\xi_6\xi_{20} T\eta - \xi_{21})}{1-\xi_1\xi_6 T^2\eta^2}\right](\delta_{wi}\cos\phi)_n$$

$$+ \left[\frac{T(1-\eta)(\xi_6\xi_{20} T\eta e^{\xi_2 T} - \xi_{21} e^{\xi_5 T}}{1-\xi_1\xi_6 T^2\eta^2}\right](\delta_{wi}\cos\phi)_{n-1} \qquad (70)$$

for $\quad n \geq 1 \cdot$ (71)

Make the definitions

$$b_1 = \left[\frac{e^{\xi_2 T} + \xi_1\xi_6 T^2(1-\eta)\eta e^{\xi_5 T}}{1-\xi_1\xi_6 T^2\eta^2}\right] \qquad (72)$$

$$b_0 = \frac{\xi_1 T\left[\eta e^{\xi_5 T} + (1-\eta)e^{\xi_2 T}\right]}{1-\xi_1\xi_6 T^2\eta^2} \qquad (73)$$

$$a_2 = \left(\frac{\xi_1 \xi_{18} T^2 \eta^2}{1-\xi_1 \xi_6 T^2 \eta^2} \right) \tag{74}$$

$$a_1 = \left[\frac{\xi_1 \xi_{18} T^2 (1-\eta) \eta e^{\xi_5 T}}{1-\xi_1 \xi_6 T^2 \eta^2} \right] \tag{75}$$

$$a_0 = \left[\frac{T\eta(\xi_{20} - \xi_1 \xi_{21} T\eta)}{1-\xi_1 \xi_6 T^2 \eta^2} \right] \tag{76}$$

$$e_3 = \left[\frac{T(1-\eta)(\xi_{20} e^{\xi_2 T} - \xi_1 \xi_{21} T\eta e^{\xi_5 T})}{1-\xi_1 \xi_6 T^2 \eta^2} \right] \tag{77}$$

$$e_2 = \left[\frac{e^{\xi_5 T} + \xi_1 \xi_6 T^2 (1-\eta) \eta e^{\xi_2 T}}{1-\xi_1 \xi_6 T^2 \eta^2} \right] \tag{78}$$

$$e_1 = \frac{\xi_6 T \left[\eta e^{\xi_2 T} + (1-\eta) e^{\xi_5 T} \right]}{1-\xi_1 \xi_6 T^2 \eta^2} \tag{79}$$

$$e_0 = \left(\frac{\xi_{18} T\eta}{1-\xi_1 \xi_6 T^2 \eta^2} \right) \tag{80}$$

$$\tau_{c4} = \left[\frac{\xi_{18}T(1-\eta)e^{\xi_5 T}}{1-\xi_1\xi_6 T^2\eta^2}\right]$$

(81)

$$\tau_{c5} = \left[\frac{T\eta(\xi_6\xi_{20}T\eta - \xi_{21})}{1-\xi_1\xi_6 T^2\eta^2}\right]$$

(82)

$$\tau_{c6} = \left[\frac{T(1-\eta)(\xi_6\xi_{20}T\eta e^{\xi_2 T} - \xi_{21}e^{\xi_5 T})}{1-\xi_1\xi_6 T^2\eta^2}\right].$$

(83)

If the approximations

$$\cos(\theta_L + \theta_P)_n \simeq \cos(\theta_L + \theta_P)_{n-1} \tag{84}$$

$$\cos(\theta_L + \theta_P)_{n-1} \simeq \cos(\theta_L + \theta_P)_{n-2} \tag{85}$$

are made and Equations (72) through (85) are substituted into Equations (69) and (70), then

$$q'_n \simeq b_1 q'_{n-1} + b_0 w'_{n-1} + a_2\cos(\theta_L + \theta_P)_{n-1} + a_1\cos(\theta_L + \theta_P)_{n-2} + a_0(\delta_{wi}\cos\phi)_n + e_3(\delta_{wi}\cos\phi)_{n-1} \tag{86}$$

and

$$w'_n \simeq e_2 w'_{n-1} + e_1 q'_{n-1} + e_0\cos(\theta_L + \theta_P)_{n-1} + \tau_{c4}\cos(\theta_L + \theta_P)_{n-2} + \tau_{c5}(\delta_{wi}\cos\phi)_n + \tau_{c6}(\delta_{wi}\cos\phi)_{n-1} \tag{87}$$

Equations (86) and (87) can each be evaluated with one line of digital program code.

Consider coupled Equations (2) and (5) together.

$$\dot{r}' = -\xi_1 v' + \xi_2 r' + \xi_{20}\, \delta_{wi} \sin\phi \tag{88}$$

$$\dot{v}' = \xi_5 v' - \xi_6 r' + \xi_{21}\, \delta_{wi} \sin\phi \tag{89}$$

Take the Laplace transforms of equations (88) and (89) and assume constant coefficients to obtain,

$$r'(s) = [r'(o) - \xi_1 v'(s) + \xi_{20} L(\delta_{wi} \sin\phi)] \,/\, (s-\xi_2) \tag{90}$$

$$v'(s) = [v'(o) - \xi_6 r'(s) + \xi_{21} L(\delta_{wi} \sin\phi)] \,/\, (s-\xi_5) \tag{91}$$

after rearrangement. The coupling is shown in Figure 3. By direct analogy with the method used on the $q'(s)$ and $w'(s)$ equations, one can find that

$$r'_n \simeq e^{\xi_2 T} r'_{n-1} - \xi_1 T\eta v'_n - \xi_1 T(1-\eta) e^{\xi_2 T} v'_{n-1} + \xi_{20} T\eta (\delta_{wi} \sin\phi)_n + \xi_{20} T(1-\eta) e^{\xi_2 T} (\delta_{wi} \sin\phi)_{n-1} \tag{92}$$

and

$$v'_n \simeq e^{\xi_5 T} v'_{n-1} - \xi_6 T\eta r'_n - \xi_6 T(1-\eta) e^{\xi_5 T} r'_{n-1} + \xi_{21} T\eta (\delta_{wi} \sin\phi)_n + \xi_{21} T(1-\eta) e^{\xi_5 T} (\delta_{wi} \sin\phi)_{n-1} \tag{93}$$

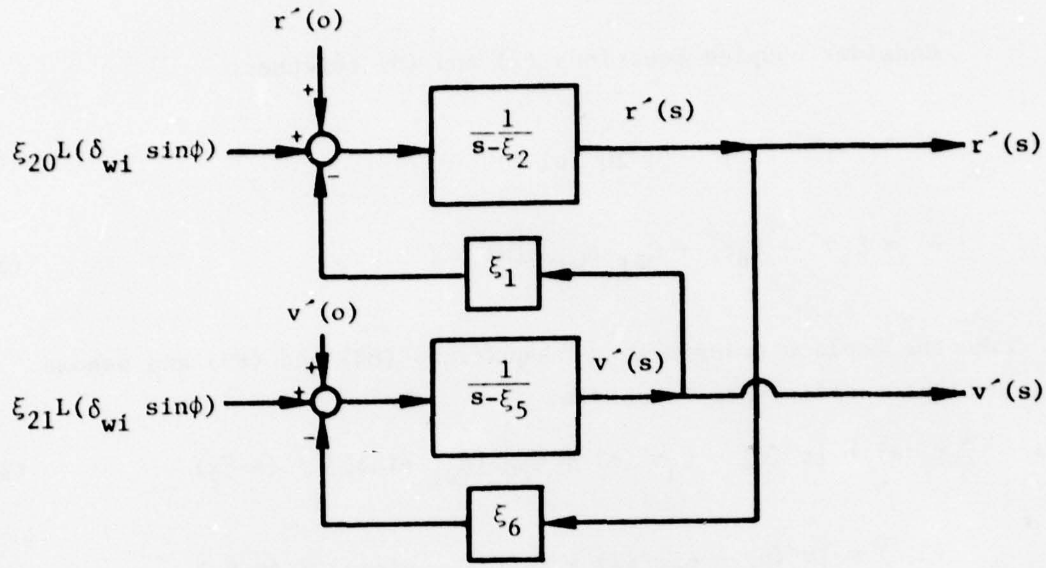

Figure 3. r´ and v´ coupling diagram.

for

$$n \geq 1 \ . \tag{94}$$

One also finds that for

$$n = 0 \tag{95}$$

that

$$r'(o) = r'(o) \tag{96}$$

and

$$v'(o) = v'(o) \tag{97}$$

are consistent with the handling of nonzero initial conditions.

Equations (92) and (93) are algebraic equations that can be solved simultaneously for r'_n and v'_n. The results are

$$r'_n \simeq \left[\frac{e^{\xi_2 T} + \xi_1\xi_6 T^2(1-\eta)\eta e^{\xi_5 T}}{1 - \xi_1\xi_6 T^2\eta^2}\right] r'_{n-1} - \frac{\xi_1 T[\eta e^{\xi_5 T} + (1-\eta)e^{\xi_2 T}]}{1 - \xi_1\xi_6 T^2\eta^2} v'_{n-1}$$

$$+ \left[\frac{T\eta(\xi_{20}-\xi_1\xi_{21}T\eta)}{1-\xi_1\xi_6 T^2\eta^2}\right](\delta_{wi}\sin\phi)_n$$

$$+ \left[\frac{T(1-\eta)(\xi_{20}e^{\xi_2 T} - \xi_1\xi_{21}T\eta e^{\xi_5 T})}{1 - \xi_1\xi_6 T^2\eta^2}\right](\delta_{wi}\sin\phi)_{n-1} \tag{98}$$

and

$$v'_n \simeq \left[\frac{e^{\xi_5 T} + \xi_1\xi_6 T^2(1-\eta)\eta e^{\xi_2 T}}{1 - \xi_1\xi_6 T^2\eta^2}\right] v'_{n-1} - \frac{\xi_6 T[\eta e^{\xi_2 T} + (1-\eta)e^{\xi_5 T}]}{1 - \xi_1\xi_6 T^2\eta^2} r'_{n-1}$$

$$+ \left[\frac{T\eta(\xi_{21} - \xi_6\xi_{20}T\eta)}{1-\xi_1\xi_6 T^2\eta^2}\right](\delta_{wi}\sin\phi)_n$$

$$+ \left[\frac{T(1-\eta)(\xi_{21}e^{\xi_5 T} - \xi_6\xi_{20}T\eta e^{\xi_2 T})}{1 - \xi_1\xi_6 T^2\eta^2}\right](\delta_{wi}\sin\phi)_{n-1} \tag{99}$$

for

$$n \geq 1 . \tag{100}$$

Substitute Equations (72), (73), (76), (77), (78), (79), (82), and (83) into Equations (98) and (99). The results are

$$r'_n \simeq b_1 r'_{n-1} - b_o v'_{n-1} + a_o(\delta_{wi} \sin\phi)_n + e_3(\delta_{wi} \sin\phi)_{n-1} \tag{101}$$

and

$$v'_n \simeq e_2 v'_{n-1} - e_1 r'_{n-1} - \tau_{c5}(\delta_{wi} \sin\phi)_n - \tau_{c6}(\delta_{wi} \sin\phi)_{n-1} \; . \tag{102}$$

Equations (101) and (102) can each be evaluated with one line of digital program code.

If Equation (30) is written with an initial condition,

$$\theta_P \simeq \int_o^t q' dt + \theta_{SE} \; . \tag{103}$$

Take the Laplace transform of Equation (103).

$$\theta_P(s) \simeq \frac{q'(s) + \theta_{SE}}{s} \tag{104}$$

Take the Z-transform of Equation (104).

$$\theta_P(z) \simeq \mathbf{Z}[q'(s)(\tfrac{1}{s})] + \theta_{SE}\,\mathbf{Z}(\tfrac{1}{s}) \tag{105}$$

Use Equation (39) and the transform table in the Appendix on Equation (105).

$$\theta_P(z) \simeq Tq'(z)(\frac{1}{1-z}) - T[\eta q'(o)(\frac{1}{1-z}) + (1-\eta)L^{-1}(\frac{1}{S})_{t=o}q'(z)] + \frac{\theta_{SE}}{1-z} \tag{106}$$

$$\theta_p(z) \simeq \frac{Tq'(z) - T\eta q'(o) - T(1-\eta)(1-z)q'(z) + \theta_{SE}}{1 - z} \tag{107}$$

$$(1-z)\theta_p(z) \simeq T\eta q'(z) + T(1-\eta)zq'(z) - T\eta q'(o) + \theta_{SE} \tag{108}$$

Applicable Z-transforms definitions are

$$\theta_p(z) = \sum_{n=0}^{\infty} \theta_p(nT)z^n \tag{109}$$

and

$$q'(z) = \sum_{n=0}^{\infty} q'(nT)z^n . \tag{110}$$

Substitute Equations (109) and (110) into Equation (108).

$$(1-z)\sum_{n=0}^{\infty} \theta_p(nT)z^n \simeq T\eta\sum_{n=0}^{\infty} q'(nT)z^n + T(1-\eta)z\sum_{n=0}^{\infty} q'(nT)z^n$$

$$- T\eta q'(o) + \theta_{SE} \tag{111}$$

$$\sum_{n=0}^{\infty} \theta_p(nT)z^n - \sum_{n=0}^{\infty} \theta_p(nT)z^{n+1} \simeq T\eta\sum_{n=0}^{\infty} q'(nT)z^n + T(1-\eta)\sum_{n=0}^{\infty} q'(nT)z^{n+1}$$

$$- T\eta q'(o) + \theta_{SE} \tag{112}$$

Use the shifting theorem, Equation (54), in Equation (112).

$$\sum_{n=0}^{\infty} \theta_p(nT)z^n - \sum_{n=1}^{\infty} \theta_p(nT-T)z^n \simeq T\eta\sum_{n=0}^{\infty} q'(nT)z^n$$

$$+ T(1-\eta)\sum_{n=1}^{\infty} q'(nT-T)z^n - T\eta q'(o)$$

$$+ \theta_{SE} \tag{113}$$

Complete all Z-transforms in Equation (113).

$$\sum_{n=0}^{\infty} \theta_p(nT)z^n - \sum_{n=0}^{\infty} \theta_p(nT-T)z^n + \theta_p(-T) \simeq T\eta\sum_{n=0}^{\infty} q'(nT)z^n$$

$$+ T(1-\eta)\sum_{n=0}^{\infty} q'(nT-T)z^n$$

$$- T(1-\eta)q'(-T) - T\eta q'(o)$$

$$+ \theta_{SE} \tag{114}$$

The ability of Equation (114) to handle a nonzero initial condition can be shown by letting

$$n = 0 \tag{115}$$

and noting that

$$\theta_p(o) = \theta_{SE} \text{ , (superelevation angle)} \tag{116}$$

results when coefficients of z^n are equated. Now let

$$n = 1 \tag{117}$$

and equate coefficients of z^n in Equation (114) to obtain,

$$\theta_p(T) \simeq \theta_p(o) + T\eta q'(T) + T(1-\eta)q'(o) \ . \tag{118}$$

Now let

$$n = 2 \tag{119}$$

and equate coefficients of z^n in Equation (114) to obtain,

$$\theta_p(2T) \simeq \theta_p(T) + T\eta q'(2T) + T(1-\eta)q'(T) \; . \tag{120}$$

Comparison of Equations (118) and (120) shows that for

$$n \geq 1 \tag{121}$$

the general recurrence equation is

$$\theta_{p_n} \simeq \theta_{p_{n-1}} + T\eta q'_n + T(1-\eta)q'_{n-1} \; . \tag{122}$$

Equation (31) can be written with an initial condition as

$$\Psi_p \simeq \int_o^t \tau_9 \, dt + \Psi_{LEAD} \; . \tag{123}$$

where

$$\tau_9 = r'/\cos\theta_p \; . \tag{124}$$

Take the Laplace transform of Equation (123).

$$\Psi_p(s) \quad \frac{\tau_9(s) + \Psi_{LEAD}}{s} \; . \tag{125}$$

If Equation (125) is treated the same as Equation (104), then

$$\Psi_{p_n} \simeq \Psi_{p_{n-1}} + T\eta\tau_{9n} + T(1-\eta)\tau_{9n-1} \; . \tag{126}$$

and

$$\Psi_p(o) = \Psi_{LEAD}, \text{ (lead angle)} \; . \tag{127}$$

Make the definitions,

$$\tau_{c1} = T\eta \qquad (128)$$

and

$$\tau_{c2} = T(1-\eta) \ . \qquad (129)$$

Substitution of Equations (128) and (129) into Equations (122) and (126) yields

$$\theta_{P_n} \simeq \theta_{P_{n-1}} + \tau_{c1} q'_n + \tau_{c2} q'_{n-1} \qquad (130)$$

and

$$\psi_{P_n} \simeq \psi_{P_{n-1}} + \tau_{c1} \ \tau 9_n + \tau_{c2} \ \tau 9_{n-1} \qquad (131)$$

for

$$n \geq 1 \ . \qquad (132)$$

Equations (130) and (131) can each be evaluated by one line of digital program code.

Now the longitudinal acceleration of the missile can be computed algebraically with the aid of Equations (1), (21), (86), (87), (101), (102), and the approximation

$$\sin(\theta_L + \theta_P)_n \simeq \sin(\theta_L + \theta_P)_{n-1} \qquad (133)$$

as

$$\dot{u}'_n \simeq \xi_{14} + v'_n r'_n - w'_n q'_n - \xi_{18} \sin(\theta_L + \theta_P)_{n-1} \ . \qquad (134)$$

Tunable integration [2] of Equation (134) yields

$$u'_n \simeq u'_{n-1} + T\eta \dot{u}'_n + T(1-\eta)\dot{u}'_{n-1} \qquad (135)$$

where

$$u'(o) = u'_{BORECLEAR} \, . \tag{136}$$

Note that the tunable integrator is in the same form as that obtained by tunable trapezoidal convolution [2] of integration of uncoupled variables. They are equivalent. Substitute Equations (128) and (129) into equation (135).

$$u'_n \simeq u'_{n-1} + \tau_{c1}\dot{u}'_n + \tau_{c2}\dot{u}'_{n-1} \tag{137}$$

Equations (134) and (137) can each be evaluated with one line of digital program code.

Finally, Equation (29) can be written with an initial condition as

$$\phi = \int_o^t p'dt + \phi_{BORECLEAR} \tag{138}$$

and treated the same as equation (103). Usually,

$$\phi_{BORECLEAR} = 0 \, . \tag{139}$$

The resulting recurrence Equation for

$$n \geq 1 \tag{140}$$

is then

$$\phi_n \simeq \phi_{n-1} + \tau_{c1}p'_n + \tau_{c2}p'_{n-1} \tag{141}$$

where

$$\phi(o) = \phi_{BORECLEAR} \, . \tag{142}$$

The p' roll rate history to be integrated must be representative of test flight conditions and be available over the missile flight time of interest.

4. DISCUSSION

Although the airframe model has been derived with the assumption of constant coefficients, it is known that the coefficients are time varying and that some have discrete jumps corresponding to wing erection and motor events. In order to minimize the error associated with such an assumption, the coefficients are updated only one-fourth as often as the airframe variables. This method allows the coefficients to appear constant for three out of every four passes through the airframe equations, but yet allows time variation and thus discrete jumps in these coefficients on the fourth pass. This approach is desirable not only because it allows stable solutions when the tunable trapezoidal convolution [2] phase parameter, η, is tuned, but also because it relieves the real time computing load by not requiring coefficient recomputation in each pass through the airframe. Passes are identified with frame numbers that cycle through one to four as shown in Figure 4. The coefficient computing load is then distributed among the four frames. This method also allows the distribution of other simulation computations in the four frames as long as real-time computing limits are not exceeded.

This airframe model has been used in three applications to date as illustrated in Figure 5. The first application was a real time hardware-in-the-loop IRSS simulation. This simulation was implemented as shown in Figures 5a and 6. The purpose of the airframe model is to drive IRSS commands that cause real time motion of the hardware-in-the-loop (guidance section). The IRSS then supplies measured hardware motion as well as guidance section output, $\delta_{wi_{n-1}}$, in order to close the simulation loop. It should be noted that the guidance section is responding to a real time projected IR environment during this time and is therefore driving the simulation when in closed loop. Note also that open loop capability is present for checkout and other studies.

The second application is to emulate the IRSS system as shown in Figure 5b. The emulation is critical to use of the IRSS simulation since it allows checkout and some validation to be accomplished without subjecting the actual guidance section to heavy wear during checkout. Also, a majority of the IRSS checkout can be emulated even when the IRSS facility [1] has frequent maintenance or other missile users. Then all lessons learned on the emulator are transferred to the IRSS program with its identical airframe.

The third application is to simulate a rolling airframe missile in a pure digital simulation as shown in Figure 5c. An effective digital seeker model is required, but extra computation spent here is offset by reduced computation in the airframe model presented. The result is a reasonably economical simulation suitable for kinematic boundary studies and other general applications. It should be noted that the seeker model used here is also used in the IRSS emulator.

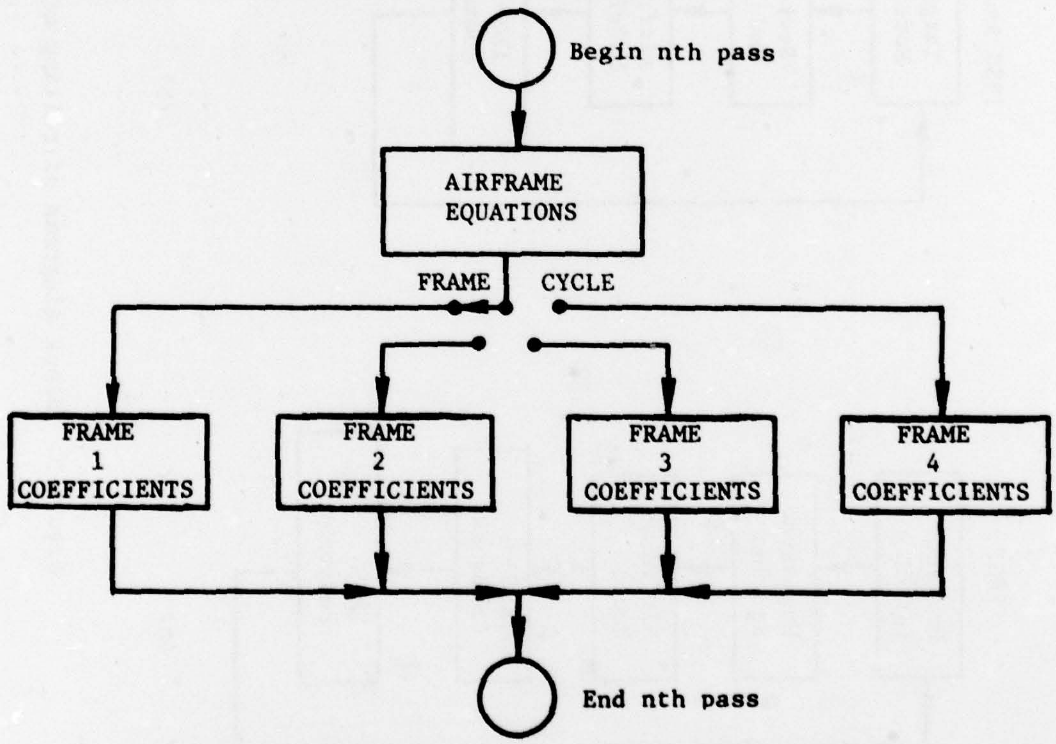

Figure 4. Airframe model calculation block diagram.

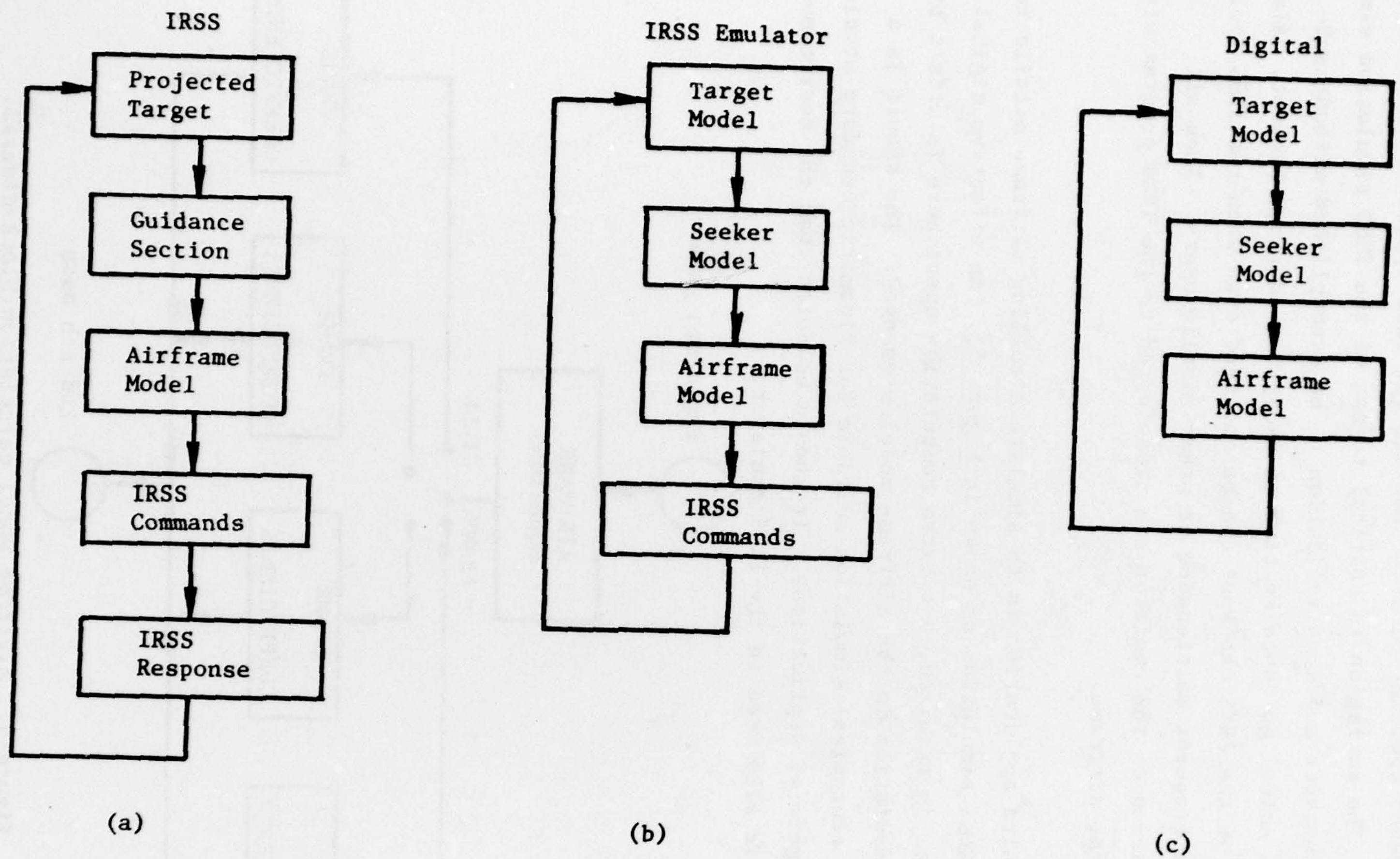

Figure 5. Block diagrams of rolling missile airframe model applications.

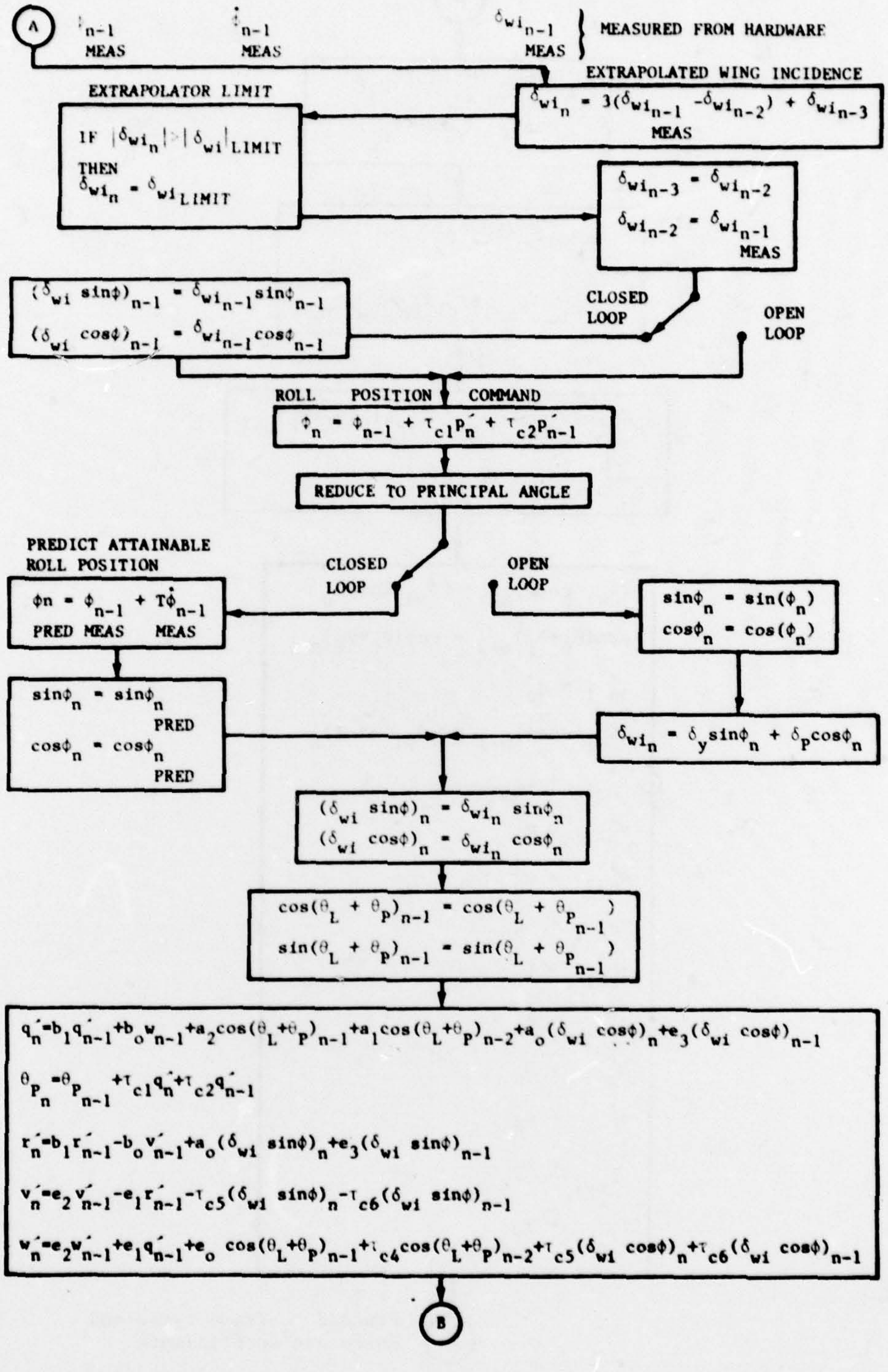

Figure 6. Airframe model implementation in the IRSS.

B

$$\sin\theta_{P_n} = \sin(\theta_{P_n})$$
$$\cos\theta_{P_n} = \cos(\theta_{P_n})$$

$$\tau_{9_n} = r'_n/\cos\theta_{P_n}$$
$$\Psi_{P_n} = \Psi_{P_{n-1}} + \tau_{c1}\tau_{9n} + \tau_{c2}\tau_{9n-1}$$

$$\dot{u}'_n = \xi_{14} + v'_n r'_n - w'_n q'_n - \xi_{18}\sin(\theta_L+\theta_P)_{n-1}$$
$$u'_n = u'_{n-1} + \tau_{c1}\dot{u}'_n + \tau_{c2}\dot{u}'_{n-1}$$

$$(\delta_{wi}\cos\phi)_{n-1} = (\delta_{wi}\cos\phi)_n$$
$$\cos(\theta_L+\theta_P)_{n-2} = \cos(\theta_L+\theta_P)_{n-1}$$
$$q'_{n-1} = q'_n$$
$$(\delta_{wi}\sin\phi)_{n-1} = (\delta_{wi}\sin\phi)_n$$
$$r'_{n-1} = r'_n$$
$$v'_{n-1} = v'_n$$
$$w'_{n-1} = w'_n$$
$$\tau_{9n-1} = \tau_{9n}$$
$$\phi_{n-1} = \phi_n$$
$$p'_{n-1} = p'_n$$
$$\dot{u}'_{n-1} = \dot{u}'_n$$
$$u'_{n-1} = u'_n$$
$$\theta_{P_{n-1}} = \theta_{P_n}$$
$$\Psi_{P_{n-1}} = \Psi_{P_n}$$

C Proceed to frame cycle and calculate coefficients

Figure 6. Airframe model implementation in the IRSS. (Continued)

APPENDIX

TABLE OF TRANSFORMS

f_o	F(t)	f(s)	f(z)
1	1	$\frac{1}{s}$	$\frac{1}{1 - z}$
0	t	$\frac{1}{s^2}$	$\frac{Tz}{(1 - z)^2}$
0	t^2	$\frac{2!}{s^3}$	$\frac{T^2\, z(1+z)}{(1 - z)^3}$
0	t^3	$\frac{3!}{s^4}$	$\frac{T^3 z(1+4z+z^2)}{(1 - z)^4}$
1	e^{-at}	$\frac{1}{s + a}$	$\frac{1}{1 - z\, e^{-at}}$
0	$t\, e^{-at}$	$\frac{1}{(s + a)^2}$	$\frac{Tz\, e^{-aT}}{(1 - z\, e^{-aT})^2}$
0	$1 - e^{-at}$	$\frac{a}{s(s + a)}$	$\frac{(1 - e^{-aT})z}{(1 - z)(1 - z\, e^{-aT})}$
b	$\frac{a}{\omega} \sin \omega t$ $+b \cos \omega t$	$\frac{a + bs}{s^2 + \omega^2}$	$\frac{b+z(\frac{a}{\omega} \sin \omega T - b \cos \omega T)}{1-2z \cos \omega T + z^2}$
0	$at+e^{-at}-1$	$\frac{a^2}{s^2(s+a)}$	$\frac{(aT+e^{-aT}-1)z+(1-e^{-aT}-aTe^{-aT})z^2}{(1-z)^2(1-z\, e^{-aT})}$
0	$1-(1+at)e^{-at}$	$\frac{a^2}{s(s+a)^2}$	$\frac{1}{1-z} - \frac{1+z\, e^{-aT}(aT-1)}{(1-z\, e^{-aT})}$
1	$\cos \omega t$	$\frac{s}{s^2+\omega^2}$	$\frac{1-z \cos \omega T}{1-2z \cos \omega T+z^2}$

TABLE OF TRANSFORMS (CONTINUED)

f_o	$f(t)$	$f(s)$	$f(z)$
0	$\sin \omega t$	$\frac{\omega}{s^2+\omega^2}$	$\frac{z \sin \omega T}{1-2z \cos \omega T+z^2}$
1	$e^{-at} \cos \omega t$	$\frac{s+a}{(s+a)^2+\omega^2}$	$\frac{1-z e^{-aT} \cos \omega T}{1-2z e^{-aT} \cos \omega T+e^{-2aT}z^2}$
0	$e^{-at} \sin \omega t$	$\frac{\omega}{(s+a)^2+\omega^2}$	$\frac{z e^{-aT} \sin \omega T}{1-2z e^{-aT} \cos \omega T+e^{-2aT}z^2}$
1	$\cosh \omega t$	$\frac{\omega}{s^2-\omega^2}$	$\frac{1-z \cosh \omega T}{1-2 z \cosh \omega T+z^2}$
0	$\sinh \omega t$	$\frac{\omega}{s^2-\omega^2}$	$\frac{z \sinh \omega T}{1-2z \cosh \omega T+z^2}$
1	$e^{-at} \cosh \omega t$	$\frac{s+a}{(s+a)^2-\omega^2}$	$\frac{z \sinh \omega T}{1-2z \cosh \omega T+z^2}$
0	$e^{-at} \sinh \omega t$	$\frac{\omega}{(s+a)^2-\omega^2}$	$\frac{z e^{-aT} \sinh \omega T}{1-2z e^{-aT} \cosh \omega T+z^2 e^{-2aT}}$
$\cos\phi$	$\cos(\omega t+\phi)$	$\frac{s \cos\phi+\omega \sin\phi}{s^2+\omega^2}$	$\frac{\cos\phi-z \cos(\omega T-\phi)}{1-2z \cos \omega T+z^2}$
$\sin\phi$	$\sin(\omega t+\phi)$	$\frac{\omega \cos\phi+s \sin\phi}{s^2+\omega^2}$	$\frac{\sin\phi+z \sin(\omega T+\phi)}{1-2z \cos \omega T+z^2}$
$\delta(o)$	$\delta(t)$	1	$\delta(o)$
$\delta'(o)$	$\delta'(t)$	s	$\delta'(o)$
$\delta^{(n)}(o)$	$\delta^{(n)}(t)$	s^n	$\delta^{(n)}(o)$
$\delta(nT)$	$\delta(t-nT)$	e^{-nst}	$z^n\delta(o)$

(This table is extracted from reference 2.)

REFERENCES

1. Grimes, V., Dublin, D. H., Johnson, J. C., Latham, J., Carter, A.L., Finley, I., and Evans, J., Open-Loop Testing of Interim Hybrid/IRSS Simulation System, US Army Missile Command, Redstone Arsenal, Alabama, September 1975, Report No. RD-76-15 (Unclassified).

2. Dickson, R. E., Tunable Integration and Tunable Trapezoidal Convolution - A Potpourri, US Army Missile Research and Development Command, Redstone Arsenal, Alabama, 5 May 1977, Report No. TD-77-12 (Unclassified).

3. Dickson, R. E., Trapezoidal Convolution Revisited: R-K Convolution or the Digital Simulation of Continuous Systems Via Z-Transforms, US Army Missile Research and Development Command, 15 June 1978, Report No. T-78-66 (Unclassified).

SYMBOLS

A_1, A_2	Curve fit functions for representing ΔC_A
C_A	Axial drag coefficient
ΔC_A	Incremental axial force coefficient
C_{DO}	Zero lift drag coefficient
Cm', Cn'	Moment and normal force coefficients
Cmw, Cnw	Control wing moment and normal force coefficients
Cm_q	Damping coefficient
Cm^*, Cn^*	Modified secant slope moment and normal force coefficients without plume effects
Cm_{pe}, Cn_{pe}	Exhaust plume effect moment and normal force coefficient increments to Cm^* and Cn^*
Cm^*_{total}, Cn^*	Total modified secant slope moment and normal force coefficients
d	Missile reference diameter
e	Base of natural logarithms
f_1, f_2, f_3, f_4	Curve fit functions for representing Cn^*
F_1, F_2, F_3, F_4	Curve fit functions for representing Cm^*
g	Acceleration due to gravity
g_1, g_2	Curve fit functions for representing Cnw_1
G_1, G_2	Curve fit functions for representing Cmw_1
I_y	Moment of inertia about y, or z axes
m	Missile roll, pitch, and yaw rates

S	Missile reference area
t	Time from missile boreclear
T_h	Missile thrust
u', v', w'	Missile velocity components
$\dot{u}'$, $\dot{v}'$, $\dot{w}'$	Missile acceleration components
X, Y, Z	Missile fixed coordinates
X_{CG}	Distance between CG and missile nose
X_R	Distance between wind tunnel reference point and missile nose
X', Y', Z'	Nonrolling missile coordinates
α	Missile angle of attack
δ_{wi}	Missile control wing incidence
θ_L, Ψ_L	Euler angles from earth fixed to launch coordinate system
θ_P, Ψ_P	Euler angles from nonrolling missile to launch coordinates
ρ	Atmospheric density
ϕ	Roll angle between missile fixed and nonrolling missile coordinate axes
ϕ'	Roll angle between missile fixed coordinate system and the projection of the missile velocity vector in the $Y'Z'$ plane
$(\ )_{\delta=0}$	At zero wing incidence
$(\ )_{t=0}$	At time from boreclear equal zero
b_1, b_0, a_2, a_1	Coefficients
a_0, e_3, τ_{c1}, τ_{c2},	
e_2, e_1, τ_{c5}, τ_{c6},	

e_0, τ_{c4}

$(\ )_n$	At present time
$(\ )_{n-1}$	At present time minus T
$(\ )_{n-2}$	At present time minus 2T
$(\ )_{n-3}$	At present time minus 3T
T	Simulation time step
$(\ )_{BORECLEAR}$	At time t = 0
η	Tuning parameter
n	Integer time step number (n = 0 @ t = 0)
θ_{SE}	Superelevation angle
Ψ_{LEAD}	Lead angle
z	Complex variable used in Z-transform definition
s	Complex variable used in laplace transform definition
$\mathcal{Z}$	Denotes the operation of taking a Z-transform
L	Denotes the operation of taking a laplace transform
L^{-1}	Denotes the operation of taking an inverse laplace transform
ξ_1, ξ_2, ξ_5, ξ_6, ξ_{18}, ξ_{20}, ξ_{21}, β_1, β_2, β_4, β_5, β_6, β_8, β_{10}, β_{11}, ξ_{14}	Utility variables and constants

DISTRIBUTION

	No. of Copies
Defense Documentation Center	
Cameron Station	
Alexandria, Virginia 22314	2
Commander	
US Army Material and Readiness Command	
ATTN: DRCRD	1
DRCDL	1
5001 Eisenhower Avenue	
Alexandria, Virginia 22333	
DRDMI-T, Dr. Kobler	1
-TBD	1
-TI (Record Copy)	1
-TI (Reference Copy)	1
DRCPM-MP, Colonel Vincent P. Defatta	1
-MPE, V. Tritt	1
DRDMI-X, Mr. McKinley	1
-TD, Dr. Grider	1
-TDF, V. Grimes	2
-TDS	1
-TEI	1
-TEO	1
-DS	1
-QS	1
Commander	
US Army Materiel Development and Readiness Command	
ATTN: DRCDE-DA (Mr. Lyle), DRCDR-WM	
Alexandria, Virginia 22333	1
Director	
Ballistics Research Laboratories	
Aberdeen Research and Development Center	
ATTN: DRXBR-VL (Mr. Mower)	
Aberdeen Proving Ground, Maryland 21005	1

No. of Copies

Commander US Army Operational Test and Evaluation Agency ATTN: CSTE-EOS (Major T. Lott) Falls Church, Virginia 22041	1
Office of the Test Director JS EO GW CM Test Program ATTN: DRXDE-TD (LTC Green) White Sands Missile Range, New Mexico 88002	1
Director US Army Materiel Systems Analysis Activity ATTN: DRXSY-ADM (Mr. Campbell) Aberdeen Proving Ground, Maryland 21005	1
Commander US Army Air Defense School ATTN: ATSA-TSM-S Ft. Bliss, Texas 79916	1
Headquarters (DAMA-WSM) Washington, DC 20310	1
Commander/Director Office of Missile Electronic Warfare US Army Electronic Warfare Laboratory ATTN: DELEW-M-ATI (Mr. Apodaca) DELEW-M-TAC (Mr. Alvarez) White Sands Missile Range, New Mexico 88002	1
Director, Development Center US Marine Corps Development and Education Command ATTN: AOD-AAW Branch Quantica, Virginia 22134	1
Commander US Army Test and Evaluation Command ATTN: DRSTE-AD (Mr. Higby) Aberdeen Proving Ground, Maryland 21005	1
Commander US Army Aviation Research and Development Command ATTN: DRCPM-ASE (Mr. Murch) St. Louis, Missouri 63166	1

	No. of Copies
Commander White Sands Missile Range ATTN: STEWS-TE-MF (Mr. Essary) White Sands Missile Range, New Mexico 88002	1